V European Conference on Computational Fluid Dynamics
ECCOMAS CFD 2010
J. C. F. Pereira and A. Sequeira (Eds)
Lisbon, Portugal, 14–17 June 2010

NON-NEWTONIAN BLOOD FLOW SIMULATION IN A REALISTIC ARTERY DOMAIN

Hasret Turkeri[*†], Senol Piskin[*], M. Serdar Celebi[*]

[*]Istanbul Technical University, Informatics Institute
e-mail: hasret.turkeri,senol.piskin@be.itu.edu.tr, mscelebi@itu.edu.tr

Key words: Non-Newtonian blood flow, Casson Model, Carreau Model, Generalised Power Law Model, carotid artery, CFD, WSS.

Abstract. *In this study, we investigate the effect of non-newtonian blood flow models on Wall Shear Stress (WSS) and velocity distribution in the artery. Three non-Newtonian viscosity models (Carreau, Casson and Generalised Power Law) [5, 12] as well as Newtonian viscosity model are used in numerical simulations. On an anatomically realistic geometry [13, 14] of a large artery obtained from actual CT or MRI data, 3D Navier-Stokes equations coupled with non-newtonian models are solved numerically. At the input of the common carotid artery, experimental flow data [3] which were obtained from a real artery bifurcation inlet are used. Numerical results on WSS and velocity distribution for each viscosity model are discussed and compared. Results indicate that the viscosity model of blood may have an impact on the numerical results especially in a real artery geometry with significant variations. Viscosity effects are relatively big for low velocity regions, and small for high velocity regions. Results obtained are compatible with the out comings of the literature on the non-newtonian blood flow simulations [5, 6, 7, 8].*

1 INTRODUCTION

The distribution of WSS in arteries is closely related to arterial diseases. CFD techniques are often used to predict the distribution of WSS. The accuracy of the CFD method is directly related to the geometric model which represents the arteries, and the blood rheology. Using anatomically realistic geometry as a computation domain makes the results more accurate compared to artificial geometry. In addition to geometric model, the rheological properties of blood have also an important effects on the results.

Several assumptions are considered for the rheological properties and the geometry in order to simplify the numerical solution of a blood flow. The most common assumption is related to the rheological properties of a blood. It is assumed that there is a linear relationship between shear rate and shear stress This is not true since the blood is a fluid which has shear thinning effects. [1, 2]

Blood viscosity depends on the shear rate, hemotocrit and temperature. For the non-Newtonian fluid model shear rate is the dominant factor that determines the viscosity. Blood has a constant viscosity over a critical shear rate, approximately$100\ s^{-1}$. Based on this fact, in many studies, blood is assumed to be a Newtonian fluid in large arteries. However, the instantaneous shear rate over a cardiac cycle changes from zero to approximately $1000\ s^{-1}$ in some large arteries [4]. This means that the assumption of Newtonian fluid may underestimate the fluid properties and behavior in blood flow simulations.

In literature, there is not any universal viscosity model which formulates the blood rheology completely. Because of the absence of such a common model, different blood viscosity models are used with various fitting parameters. Casson, Carreau and Generalised Power Method are the most common used non-Newtonian blood flow models todays.

In this study, the effect of non-Newtonian properties of blood is investigated in an anatomically realistic carotid artery bifurcation model.

The effects of non-Newtonian fluid flow are carried out by different researchers in a non-planar branch [7,8], experimental and numerical studies with a blood analog fluid [9], distal end-to-side vascular bypass anastomosis [10] and distal vascular graft anastomoses [11]. All these studies indicate that, at low shear rate ranges, the importance of non-Newtonian constitutive models is significant.

Five non-Newtonian models, Casson, Carreau, Generalised Power Method, Power Method and Walburn-Schneck, were used and compared based on WSS distribution in a steady-state simulation [5]. Initial results reveal that for a low central inlet velocity, WSS values of non-Newtonian models are higher than that of Newtonian. In the case of high central inlet velocity, WSS values of non-Newtonian and Newtonian models are nearly identical while the WSS of Power Law and Walburn-Schneck are lower than that of others. In the subsequent study of these authors, Generalised Power Method and Newtonian method were compared in transient simulation [6]. Results show that the difference between distributions of WSS in Generalised Power Method and Newtonian Method is relatively small.

2 METHODS

The behavior of the fluid is defined by 3D incompressible, time-dependent Navier-Stokes equations. The flow is assumed to be unsteady and laminar.

For blood viscosity, three non-Newtonian models, namely Carreau, Casson and Generalised Power Method are used.

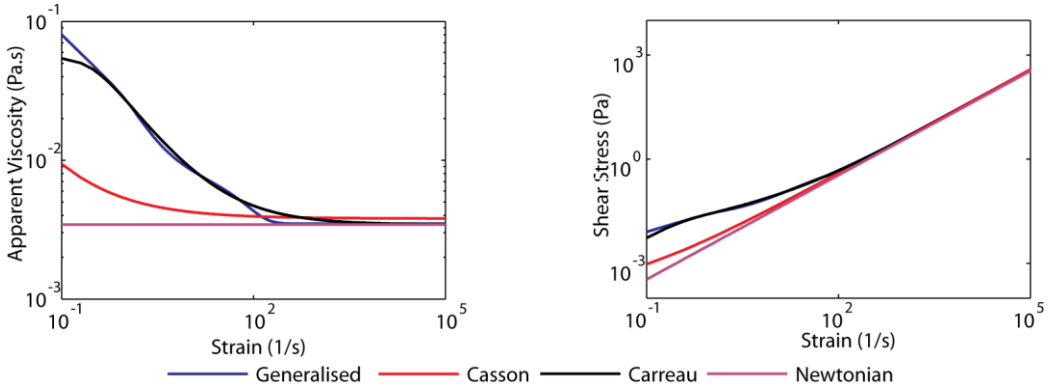

(a) Viscosity (b) Shear Stress

Figure 1: Apparent viscosity or shear stress as a function of strain

As it can be seen in Figure 1.a, the Generalized Power Method has greater viscosity at low shear rate. The viscosity of Carreua and GPM models are close to each other for shear rate values over 0.2s. For high shear range, the GPM and Carreau models converge to a limiting value which is Newtonian viscosity. On the other hand, the viscosity of Casson model is smaller than that of others at low strain rate and above that of other models at high shear rates and it does not converge to the Newtonian viscosity at high shear rates. Figure 1.b shows that the shear stresses for non-Newtonian models are higher at low strain values. Furthermore, above $100\ s^{-1}$ the shear stress of non-Newtonian models converge to the Newtonian model.

The Carreau model takes both μ_0 and μ_∞ into accounts to consider the limiting values of viscosity where μ_0 is limiting viscosity while shear rate tend to zero and μ_∞ is the limiting viscosity while shear rate goes to infinite. The form of Carreau and its parameter have been taken from [4].

$$\mu = \mu_\infty + (\mu_0 + \mu_\infty)\left[1+(\lambda\dot{\gamma})^2\right]^{(n-1)/2} \tag{1}$$

where $\lambda = 3.313s$, $n = 0.3568$, $\mu_0 = 0.56$ P and $\mu_\infty = 0.0345$ P.

The Casson model considers also the hematocrit. In human blood hemotocrit has a rate about 40-45%. The form and the fitting parameter for Casson Model is

$$\mu = \left[(\eta^2 J_2)^{1/4} + 2^{-1/2}\tau_y^{1/2}\right]^2 J_2^{-1/2} \tag{2}$$

where $|\dot{\gamma}| = 2\sqrt{J_2}$, $\tau_y = 0.1(0.625H)^3$ and $\eta = \eta_0(1-H)^{-2.5}$ with $\eta_0 = 0.012$ P and $H = 0.37$ [12].

The Generalized Power Method can be assumed as a general model of non-Newtonian viscosity. The viscosity of Generalised Power Method and Carreau method also agree well. Using the form and fitting parameter of Ballyk [1],

$$\mu = \lambda|\dot{\gamma}|^{n-1} \tag{3}$$

$$\lambda(\dot{\gamma}) = \mu_{\infty} + \Delta\mu \exp\left[-\left(1 + \frac{|\dot{\gamma}|}{a}\right) \exp\left(\frac{-b}{|\dot{\gamma}|}\right)\right] \tag{4}$$

$$n(\dot{\gamma}) = n_{\infty} - \Delta n \exp\left[-\left(1 + \frac{|\dot{\gamma}|}{c}\right) \exp\left(\frac{-d}{|\dot{\gamma}|}\right)\right] \tag{5}$$

where $\mu_{\infty} = 0.035$ P, $n_{\infty} = 1.0$, $\Delta\mu = 0.25$, $\Delta n = 0.45$, $a = 50$, $b = 3$, $c = 50$ and $d = 4$.

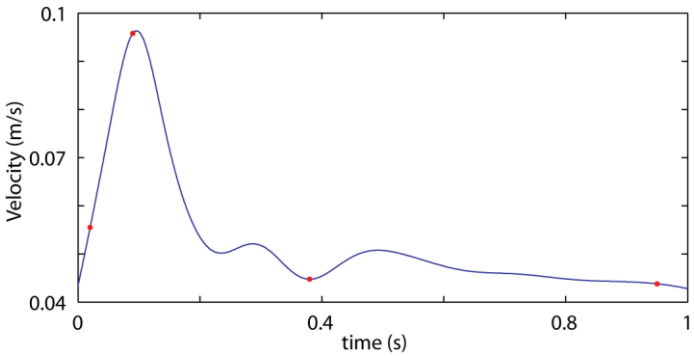

Figure 2: Inlet Velocity Profile

At the input of the common carotid artery, Womersly velocity profile which fits the experimental flow data [3] which were obtained from a real artery bifurcation is used. In Figure 2 the inlet velocity profile, where its period is one second, is shown. The geometry of the common carotid artery is anatomically realistic, a series of techniques are implemented to extract the actual artery from CT or MRI images of a patient using the Mimics Software [13, 14]. The vessel wall is assumed as rigid and no-slip boundary conditions are implemented on the wall. The simulation is done for four periods where the period of flow is one second. The results of fourth period are compared and discussed in the following section.

3 RESULTS

3.1 Main Carotid Bifurcation

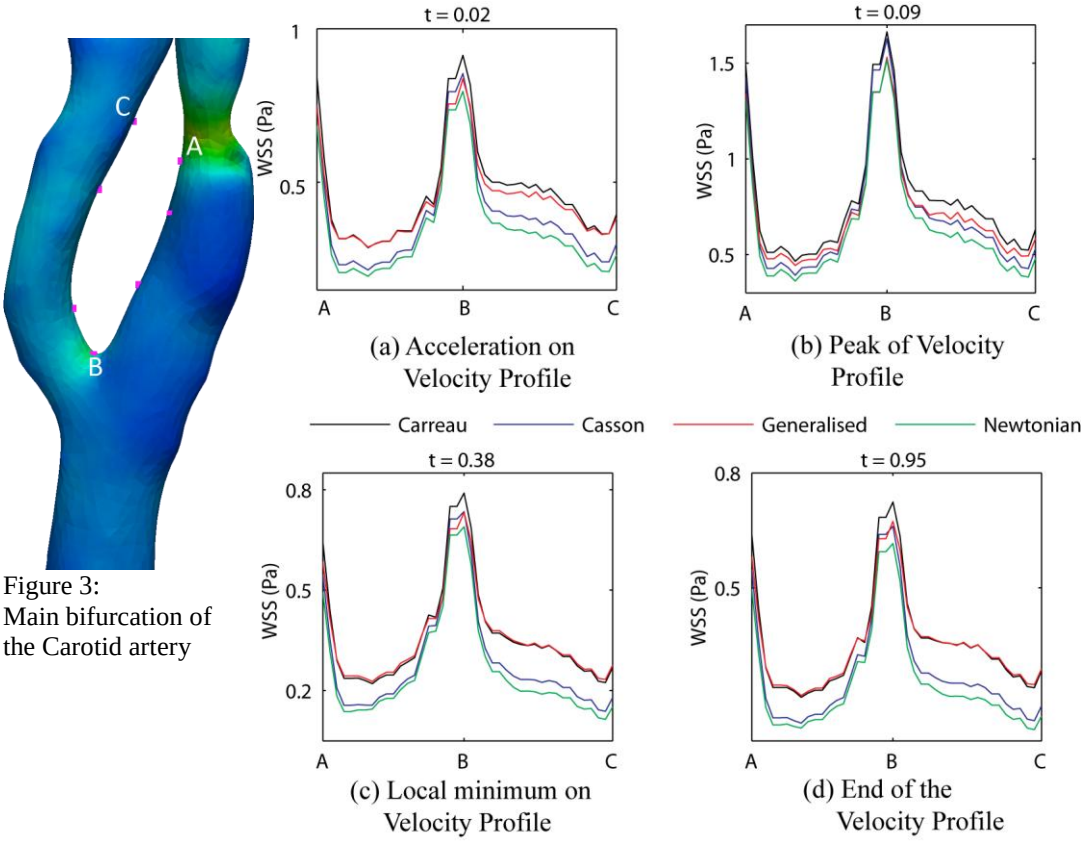

Figure 3: Main bifurcation of the Carotid artery

Figure 4: WSS distributions of various viscosity models

In Figure 4, the WSS distributions of different viscosity models at different time steps are presented. On the main bifurcation of carotid artery, the maximum WSS occurs on the stagnation point because of the high velocity gradient. Moreover, the relative differences with non-Newtonian and Newtonian models are minimum on this point due to the high shear rates. On the stagnation point, the Carreau model gives the highest WSS values at all time steps. In this region, Generalised Power Method and Carreau models have very close results. However, on the stagnation point, the difference between the results of Carraeu and Generalised Power models is increased significantly. Furthermore, the Casson model causes WSS distribution that is similar to the Newtonian model. The difference between the Casson and Newtonian models is increased on the stagnation point but the rate of difference is remained unchanged.

	Newtonian					
	Maximum		Minimum		Mean	
Carreau	58.7%	0.159 Pa	13.9%	0.058 Pa	38%	0.095 Pa
Generalised	58.6%	0.13 Pa	2.7%	0.02 Pa	33%	0.12 Pa
Casson	14.9%	0.07 Pa	5.8%	0.02 Pa	10%	0.04 Pa

Table 1: Differences between the results of non-Newtonian models and Newtonian model

Table 1 shows the maximum, minimum and mean value of the difference and the relative difference. The values in the Table 1 is calculated from simulations at t=0.02 sec. of period. From Table 1, it can be seen that, despite of small quantitative difference in WSS, the rates of difference which are up to 59% are significant,

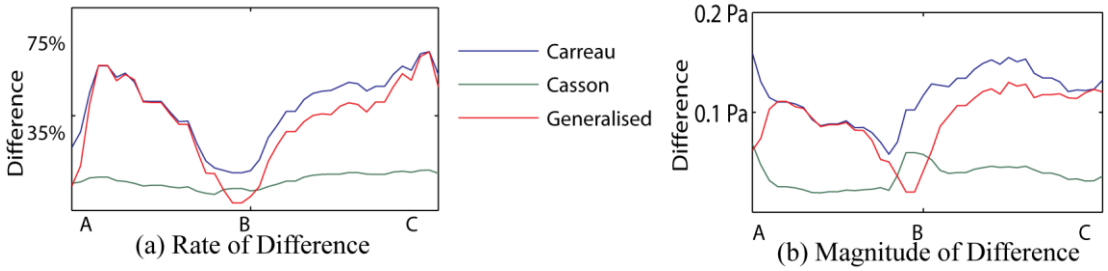

Figure 5: Difference rate and magnitude of WSS distributions

Figure 5 show the differences and the rates of difference at the path which span from A to C. The rate of difference is the minimum at the stagnation point because of high strain rates. Moreover, the Generalised Power Method gives closer results to that of Newtonian model at the high shear rates. The rate of difference between the Casson model and Newtonian has same the tendency along the path from A to C.

3.2 Carotid Sinus

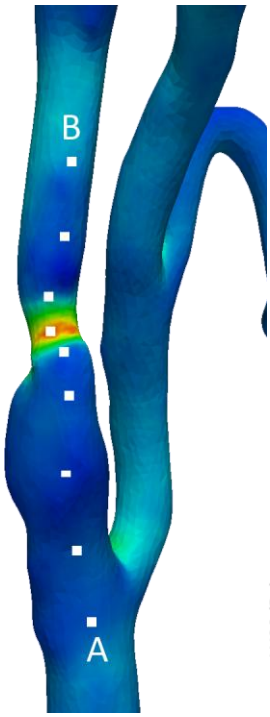

Figure 6: Carotid Sinus

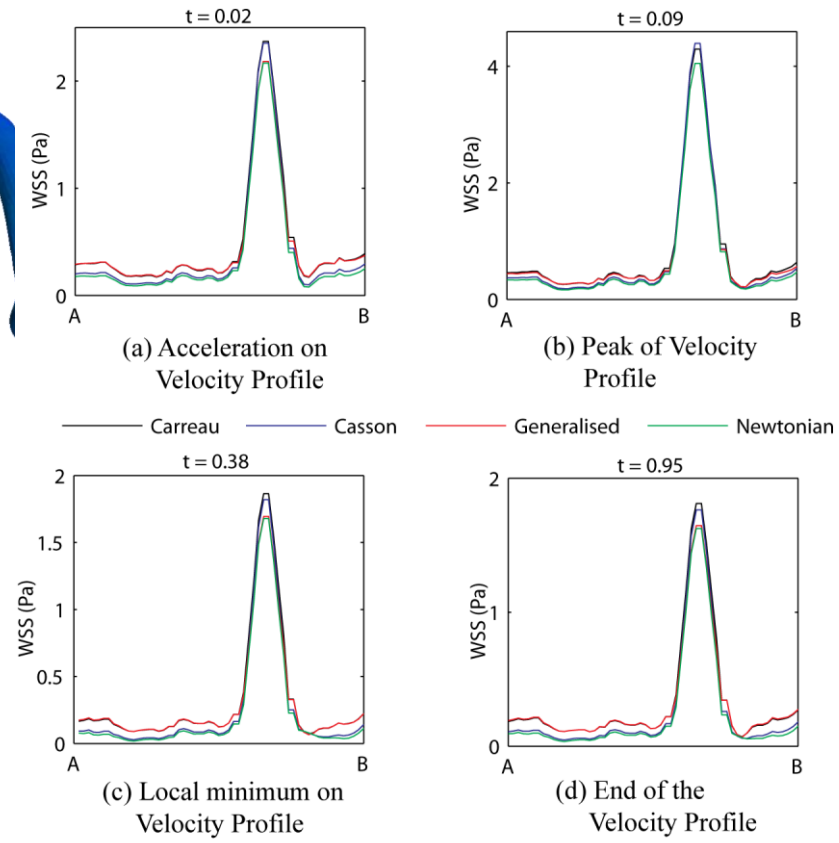

Figure 7: WSS distributions of various viscosity models

At the sinus region of internal carotid artery, WSS increases as the artery gets narrower and reaches its biggest effect at the narrowest zone. The difference between non-Newtonian and Newtonian effects is the minimum in this zone which has the maximum WSS. While the artery enlarges after the narrowest region, the value of WSS decreases rapidly. On the other hand, the difference between non-Newtonian and Newtonian effects increases rapidly. The Carreau and Generalised Power Method generally give similar WSS distribution, but at the peak point of WSS, the results of Generalised Power Method move away from the results of Carreau and get close to the

results of Newtonian. The Casson model is a non-Newtonian model which generally results lowest WSS values. However, on the peak values of WSS, the Generalised Power Method gives lower values than that of the Casson. Moreover, the Casson and the Newtonian model results show that the rate of difference in WSS distribution is not significantly change in the region spanning from A to B.

	Newtonian					
	Maximum		Minimum		Mean	
Carreau	123.5%	0.203 Pa	9.3%	0.07 Pa	60.6%	0.12 Pa
Generalised	130.1%	0.142 Pa	0.4%	0.006 Pa	60.2%	0.09 Pa
Casson	26%	0.185 Pa	8.5%	0.02 Pa	15.15%	0.04 Pa

Table 2: Differences between the results of non-Newtonian models and Newtonian model

Table 2 shows that the Generalised Power Method has the maximum and the minimum rate of difference. At the Carotid Sinus the rate of difference is up to 130%. The mean and maximum value of rate of difference of Carreau and Generalised Power Method are close.

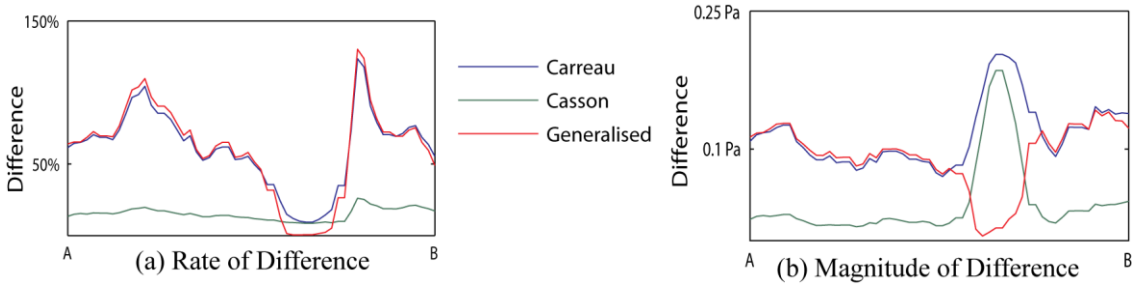

Figure 8: Difference rate and magnitude of WSS distributions

The rate and magnitude of difference along the path spanning from A to B are shown in the Figure 8. The Carreau and Generalised Power Method have the same tendency in the rate of difference, but the magnitude of difference of these two models differs on the point which has the maximum WSS. While the difference between Carreau and Newtonian increases, the difference between Generalised Power Method and Newtonian decreases at that point.

3.3 Common Carotid

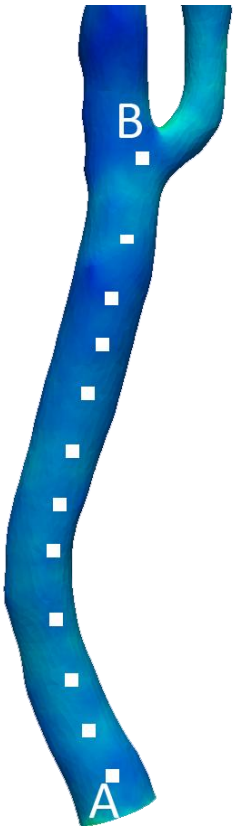

Figure 9:
Common Carotid

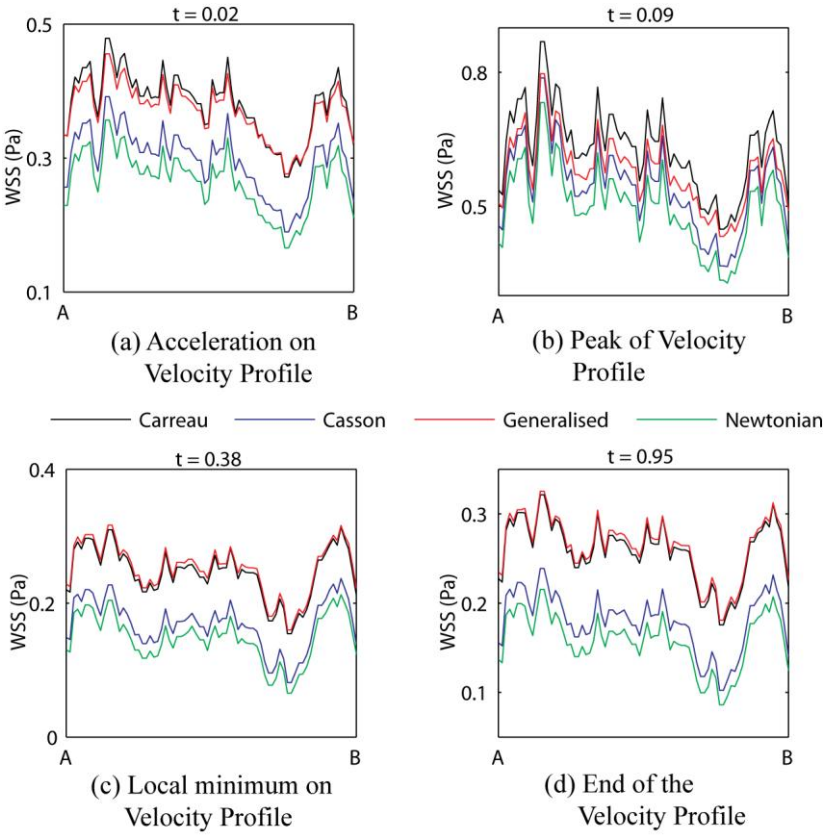

Figure 10: WSS distributions of various viscosity models

Since the radius in the Common Carotid artery does not change very much and the artery has not any significant increase on curvature, the WSS distribution along the artery does not exhibit a big change. On the path spanning from A to B, the Carreau and Generalised Power Methods give higher WSS distribution than that of Newtonian. Furthermore, the differences of both Carreau and Generalised Power Method with Newtonian model are small. The Casson model gives the lowest WSS distribution in this region. At the highest inlet velocity (see Figure 10.b), the WSS distribution of each model gives closer results which are an expected behavior of the non-Newtonian models.

	Newtonian					
	Maximum		Minimum		Mean	
Carreau	63.9%	0.128 Pa	34.3%	0.103 Pa	44.5%	0.116 Pa
Generalised	66.7%	0.122 Pa	27.7%	0.093 Pa	41.3%	0.106 Pa
Casson	14.6%	0.038 Pa	9.8%	0.02 Pa	11.8%	0.031 Pa

Table 3: Differences between the results of non-Newtonian models and Newtonian model

Table 3 shows the value of rate of difference and the magnitude of difference at the Common Carotid. Although the Generalised Power Method has the maximum rate of difference, the biggest mean rate of difference is belong to Carreau. The smallest rate of difference occurs between Casson and Newtonian.

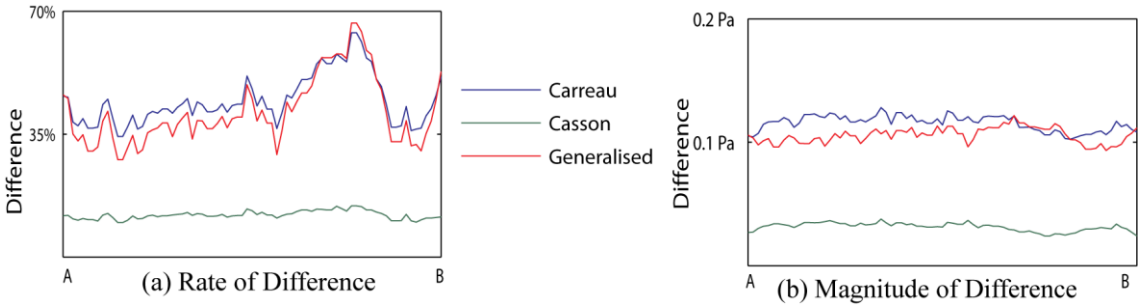

Figure 11: Difference rate and magnitude of WSS distributions

Figure 11 shows that, despite the fact that the magnitudes of differences along the path spanning from A to B have not significant changes, the rates of differences have big changes (see Figure 11.a) except the Casson model.

3.4 Velocity Profiles of Main Bifurcation

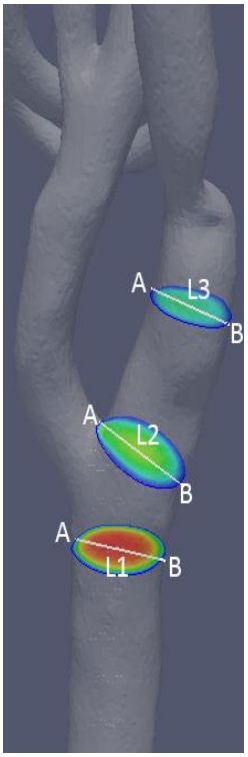

Figure 12: Lines

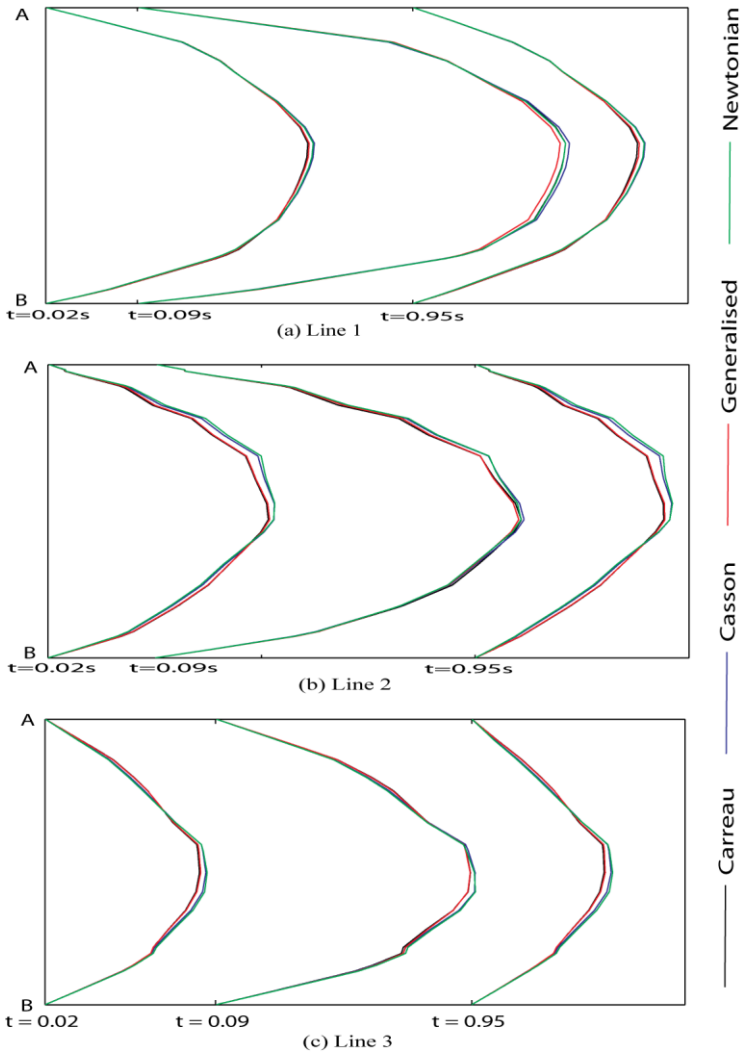

Figure 13: Velocity profiles of various viscosity models

In this section the effects of non-Newtonian properties on velocity profiles are discussed. To assess this effect, the velocity profiles along three lines inside the artery are compared.

Velocity profiles of non-Newtonian and Newtonian model simulations are studied on three distinct lines inside the artery. The first of these lines, L1, is located right before the main bifurcation, the second line, L2, is on both the main bifurcation and entrance of internal carotid artery, and the last line, L3, is located on the largest zone of the carotid sinus (see Figure 12).

Due to the lower shear rate on the centre-line of the artery, the non-Newtonian properties are dominant in this region. Because, the shear rate near the artery walls is higher, the impact of non-Newtonian effects is not dominant on velocity profiles on this region. As it can be seen in the Figure 13, while the velocity profile of a Newtonian model is paraboloid, the non-Newtonian models cause flatter velocity profiles according to shear-thinning properties of non-Newtonian models. Furthermore, the differences between non-Newtonian and Newtonian models are greater in the centre-line. Generally the Carreau and the Generalised Power Methods are in the same tendency.

The comparison of the velocity profiles on L1, L2 and L3 lines indicates that the bigger velocity gradient from A to B results an increment of non-Newtonian properties. In L1 line, the velocity gradient is smaller and velocity profile is smoother then the values of difference rate under 5%. Moreover, in the L2 line, the value of difference rate is about 20% because of the higher velocity gradient and the rougher velocity profile. Figure 14 shows the differences and the differences rate with non-Newtonian and Newtonian models.

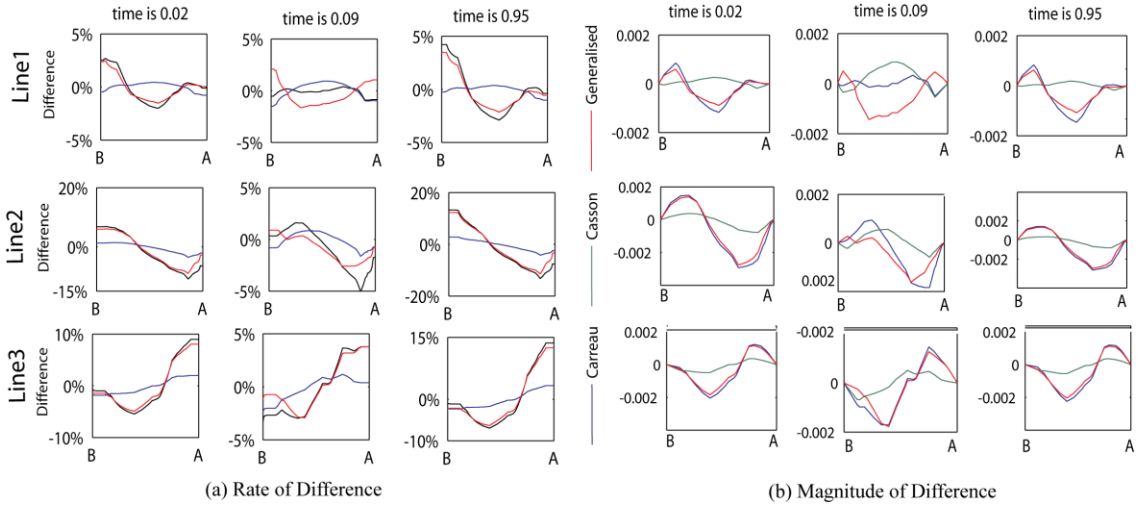

Figure 14: Differences between non-Newtonian and Newtonian on Velocity Profiles

4 CONCLUSION

In blood flow simulations with low Reynolds number, the importance of non-Newtonian properties are effected by some factors. One of these factors is the geometrical properties of the artery. At the bifurcation and narrowing zones of arteries, the non-Newtonian effects are small due to the high shear rate at these regions. Another factor is the magnitude of an instantaneous velocity at the velocity inlet profile. For example, at t=0.09 sec. the velocity profile has maximum value so, the differences between non-Newtonian and Newtonian models are minimum.

On the other hand, no big differences on the velocity profiles of non-Newtonian and Newtonian are appeared and the maximum effect of non-Newtonian properties are observed on the center-line of the vessel according to the lower shear rate.

The Carreau and the Generalised Power Method generate higher viscosity at lower shear rates thus, these two models predict higher WSS distribution than that of the Newtonian model. But, at higher shear rates, the results of the Generalised Power

Method converged to the results of Newtonian more quickly than the Carreau model. This feature is directly related to the mathematical formulation of the Generalised Power Method and the Carreau model.

The Casson model predicts lower WSS values than the other non-Newtonian models because at low and middle shear rates its viscosity smaller than those of the Carreau and the Generalised Power Method as it can be seen in the figure of apperant viscosity. At high shear rates the viscosity of Casson is a little above of the Newtonian viscosity and it does not converge to the Newtonian viscosity. As a result of this at the region with high shear rates the difference rate does not decrease while the difference of the others decreases.

ACKNOWLEDGEMENT

Computing resources used in this work were provided by the National Center for High Performance Computing of Turkey (UYBHM).

REFERENCES

[1] P. D. Ballyk, D. A. Steinman, and C. R. Ethier, Simulation of Non-Newtonian Blood Flow in an End-to-Side Anastomosis. *Biorheology*, **31**, pp. 565–586 (1994)

[2] M. K. Sharp , G. B. Thurston, and J. E.Jr. Moore, The Effect of Blood Viscoelasticity on Pulsatile Flow in Stationary and Axially Moving Tubes. *Biorheology*, **33**, pp. 185–208 (1996)

[3] S. Piskin, M. S. Celebi, A Carotid Artery Bifurcation Model for Blood Flow, 7th Int Symp On Fluid Control, Measurement and Visualization (FLUCOME '03), Sorrento, Italy, August 25-28, (2003)

[4] Y. I. Cho and K. R. Kensey, Effects of the non-Newtonian viscosity of blood on hemodynamics of diseased arterial flows: part 1, steady flows, *Biorheology*, **28**, pp. 241- 262 (1991)

[5] B. M. Johnstona, P. R. Johnstona, S. Corneyb and D. Kilpatrick, Non-Newtonian blood flow in human right coronary arteries: steady state simulations, Journal of Biomechanics, **37**, pp. 709-720 (2004)

[6] B. M. Johnstona, P. R. Johnstona, S. Corneyb and D. Kilpatrick, Non-Newtonian blood flow in human right coronary arteries: Transient simulations, Journal of Biomechanics, **39**, pp. 1116-1128 (2006)

[7] J. Chen and X. Lu, Numerical investigation of the non-Newtonian pulsatile blood flow in a bifurcation model with a non-planar branch, Journal of Biomechanics, **39**, pp. 818-832 (2006)

[8] J. Chen and X. Lu, Numerical investigation of the non-Newtonian pulsatile blood flow in a bifurcation model with a non-planar branch, Journal of Biomechanics, **37**, pp. 1899-1911 (2004)

[9] F.J.H. Gijsen, F.N. van de Vosse and J.D. Janssen, The influence of the non-Newtonian properties of blood on the flow in large arteries: steady flow in a carotid bifurcation model, **32**, pp. 601-608 (1999)

[10] S. O'Callaghan, M. Walsh and T. McGloughlin, Numerical modeling of Newtonian and non-Newtonian representation of blood in a distal end-to-side vascular bypass graft anastomosis, Medical Engineering & Physics, **28**, pp.70-74 (2006)

[11] J. Chen, X. Lu and W. Wang, Non-Newtonian effects of blood flow on hemodynamics in distal vascular graft anastomoses, Journal of Biomechanics, **39**, pp. 1983-1995 (2006)

[12] Y.C. Fung Biomechanics: mechanical properties of living tissues, 2th Edition, Springer-Verlag, (1993)

[13] S. Piskin, E. Aribas and M. S. Celebi, Coupled Simulation of a Carotid Artery Bifurcation Model, 10th Mesh Based parallel Code Coupling Interface User Forum, Sankt Augustin, Germany, February 17-18, (2009)

[14] E. Aribas, S. Piskin, M. S. Celebi, 3D blood flow simulation in human arterial tree bifurcations, 14th National Biomedical Engineering Meeting, 2009 (BIYOMUT 2009), 20-22 May (2009)